General Disclaimer

One or more of the Following Statements may affect this Document

- This document has been reproduced from the best copy furnished by the organizational source. It is being released in the interest of making available as much information as possible.

- This document may contain data, which exceeds the sheet parameters. It was furnished in this condition by the organizational source and is the best copy available.

- This document may contain tone-on-tone or color graphs, charts and/or pictures, which have been reproduced in black and white.

- This document is paginated as submitted by the original source.

- Portions of this document are not fully legible due to the historical nature of some of the material. However, it is the best reproduction available from the original submission.

TECHNICAL REPORT

A LITERATURE REVIEW ON FATIGUE AND CREEP INTERACTION

by

Wen-Ching Chen

Sponsored by:

NATIONAL AERONAUTICS AND SPACE ADMINISTRATION

NASA Grant No.: NCR 33-022-157

GEORGE SACHS FRACTURE AND FATIGUE RESEARCH LABORATORY

SYRACUSE UNIVERSITY

DEPARTMENT OF CHEMICAL ENGINEERING AND MATERIALS SCIENCE

SYRACUSE NEW YORK 13210

TECHNICAL REPORT

A LITERATURE REVIEW ON FATIGUE AND CREEP INTERACTION

by

Wen-Ching Chen

Sponsored by:

NATIONAL AERONAUTICS AND SPACE ADMINISTRATION

NASA Grant No.: NGR 33-022-157

George Sachs Fracture and Fatigue Research Laboratory
Syracuse University
Department of Chemical Engineering and Materials Science
Syracuse, New York 13210

MTS-HWL-4116-776

ACKNOWLEDGEMENT

The author is indebted to the National Aeronautics and Space Administration for sponsoring this study through the Contract No. NASA-NGR-33-022-157. The author also wishes to express his sincerest thanks to his advisor, Dr. H. W. Liu for his constant guidance and encouragement during the course of this study. Thanks are also due to Mr. H. Turner for her help in typing this manuscript.

A LITERATURE REVIEW ON FATIGUE AND CREEP INTERACTION

In the last few years, the urgent needs of material information in the designs of nuclear power plant, aircraft jet engine, and gas turbine components have prompted rapid progress in the study of fatigue-creep interaction. In dealing with fatigue-creep interaction, we generally consider the situation of fatigue at elevated temperature, which is a very comlex subject strongly affected by temperature, frequency, hold time, mean stress, and environment. Since elevated-temperature fatigue testing is rather time-consuming and expensive, estimates of the performance of specific material of engineering interest are very useful, especially in the early stage of design and material selection. At present, many life-time prediction methods, which are based on a number of empirical and phenomenological relationships, have been successfully proposed. The following three aspects are reviewed: effects of testing parameters on high-temperature fatigue, life-time prediction, and high-temperature fatigue crack growth.

EFFECTS OF TESTING PARAMETERS ON HIGH-TEMPERATURE FATIGUE:

When the temperature is raised into the region where creep becomes significant, temperature- and time-dependent effects on fatigue life should be considered. The principal parameters are: temperature, frequency, hold time and environment.

A. TEMPERATURE EFFECTS:

At a given applied stress, an increase in temperature generally reduces the number of cycles to crack initiation and the number of cycles to failure. Often the reduction in failure life is accompanied by a transition from transgranular to intergranular cracking. (1) The mecha-

nical strengths, including the fatigue strength, of materials usually decline with an increasing temperature.

B. FREQUENCY EFFECTS:

At low temperature, there is little or no effect on fatigue properties due to cyclic frequency. Only at elevated temperatures, time-dependent effects become significant. A decrease in frequency generally reduces the number of cycles to crack initiation and the number of cycles to failure. The lower the frequency is, the more the time is available for creep and oxidation. Both are deleterious to fatigue life at elevated temperature. The reduction of frequency tends to promote the intergranular cracking, which often accompanies the decrease of fatigue life. (2,3)

C. HOLD TIME EFFECTS:

Krempl and Wundt (4) have made a detailed survey on hold time effects in high-temperature low-cycle fatigue. It can be summarized as follow:

(a). An introduction of hold time generally reduces the number of cycles to failure and increases the time to failure.

(b). The hold time effects at low strain range are more pronounced than those at high strain range.

(c). An increase in hold time generally decreases the failure life, however, the saturation of hold time effects may occur for some cases.

(d). The hold time effects are more pronounced in push-pull test than in bending test.

(e). An increase in hold time favors the transition from transgranular to intergranular cracking.

(f). The effects of hold time at other than the maximum tensile position of the cycle may be either less severe or more severe than the ones at

the maximum tensile position of the cycle.

(g). The introduction of hold times leads to about the same percentage reduction of the failure lives in air and in vacuum.

D. ENVIRONMENT EFFECTS:

Even at room temperature, air may have a pronounced influence on fatigue life. At elevated temperature the environmental effects are even more so. The chief concern of environmental effects at elevated temperature is oxidation. The effects of oxidation on surface crack initiation and propagation may be advantageous or deleterious. (5)

LIFE PREDICTION METHODS:

In recent years, many life-prediction methods have been proposed. Before reviewing these methods, it is necessary to make a clear distinction between low- and high-cycle fatigue. Most of these methods deal with the low-cycle category. Some researchers prefer to designate arbitrarily, "low-cycle fatigue" as the one with a failure life less than 10^5 cycles, and "high-cycle fatigue" greater than 10^5 cycles. (2,6) Some prefer to regard high-cycle fatigue as implying that the plastic strain anywhere in a structure which is under cyclic straining, is very small, except at those discontinuities such as scratches, inclusions, notches, or joints, where localized plastic deformation may take place, and an elastic (or small scale yielding) analysis satisfactorily describes the behavior of the structure; while low-cycle fatigue implies that externally imposed high plastic strain exists in the critical portions of the structure. Others prefer to make this distinction based on the transition fatigue life in the plot of $\log \Delta\varepsilon$ vs. $\log N_f$, below the transition life is the low-cycle fatigue region and beyond that is the high-cycle fatigue region.

The demarcation is important not only in the determination of the analytical method but also in the consideration of the test method to be used in the material evaluation. The stress controlled experiments are often more convenient in the high-cycle region, while strain controlled experiments are often more meaningful in the low-cycle region.

The principal concern in formulating a criterion for fatigue life-prediction at elevated temperature is how to account for the damage caused by the time- and temperature-dependent variables. As the temperature is raised, time-dependent factors become important. This implies that the fatigue life will be affected by frequency and hold time, which in turn will affect the damage incurred by creep deformation and corrosion. There are two categories in the life-prediction methods: (a) determining the cyclic- and time-dependent damages separately, and summing them by the assumption of a linear fatigue-creep interaction; and (b) considering the cyclic- and time-dependent factors together, such as in the frequency-modification approach and the strainrange partitioning approach.

A. DAMAGE SUMMATION METHOD:

This method combines the damage summation laws of Miner (7) and Robinson (8), and was first proposed by Taira (9). The linear life fraction damage rule is recommended by the ASME Boiler and Pressure Vessel Code Case 1592.(10) Creep and fatigue damages are calculated using the following equation:

$$\sum_{j=1}^{p} \left(\frac{n}{N_d}\right)_j + \sum_{k=1}^{q} \left(\frac{t}{T_d}\right)_k \leq D \qquad (1)$$

where D = total fatigue-creep damage,

n = number of applied cycles of loading condition j, which is specified by both strain and temperature.

N_d= number of design allowable cycles (or the actual failure life) at the cyclic loading condition j,

t = accummulated hold time of the loading condition k,

T_d= time to rupture at the loading condition k.

In this method, it is assumed that the damage in creep is effectively the same as the damage in fatigue, and that the life is used up when the damage summation equals the factor, D. The fatigue damage term, $\Sigma(\frac{n}{N_d})$, is the ratio of fatigue life in the hold time test to the fatigue life in a comparable no hold time test. The creep term, $\Sigma(\frac{t}{T_d})$, is the ratio of the accummulated hold time under a given stress to the time to rupture under the same stress. If the linear life fraction concept is valid and no fatigue-creep interaction occurs, the value of D should be close to unity. A deviation from unity may indicate the interaction of fatigue and creep.

The stress relaxation is always occurred during the hold period in a strain-controlled fatigue test at elevated temperature. It is not appropriate to estimate the creep damage fraction during the hold periods based on a constant stress. Gittus (11) presented an equation to deal with stress relaxation during a hold period

$$\ln(\sigma_o/\sigma) = A/1+m \cdot t^{1+m} \qquad (2)$$

where σ_o is the initial (maximum) stress, σ the instantaneous stress at time t, and A and m constants. Both Campbell (12) and Jaske et al.(13) have confirmed this viewpoint and calculated the creep damage fraction by a numerical integration of $\int_o^t \frac{dt}{T_d}$ to account for the stress relaxation during the hold period. In this integration of $\int_o^t \frac{dt}{T_d}$, the information of the stress relaxation curve and the creep-rupture curve of the material at the testing condition are needed.

Recently, Langeborg and Attermo (14) showed that a linear fatigue-creep damage rule did not apply to their experiments on 20Cr-35Ni stainless steel subjected to cyclic reversed bending strains and a constant tensile load. They introduced the hold time at the zero strain and thus induced a creep on the specimen during the hold period. The introduction of an interaction term, which is the product of the fatigue damage and creep damage, to the linear damage rule then adequately accounts for the observed lives.

$$\frac{N_f}{N_{f_o}} + B \cdot \left(\frac{N_f}{N_{f_o}} \cdot \Sigma \frac{t_i}{t_{f_o}}\right)^{1/2} + \Sigma \frac{t_i}{t_{f_o}} = 1 \qquad (3)$$

or

$$\frac{N_f}{N_{f_o}} + B \cdot \left(\frac{N_f}{N_{f_o}} \cdot \frac{N_f \cdot 2t_i}{t_{f_o}}\right)^{1/2} + \frac{N_f \cdot 2t_i}{t_{f_o}} = 1$$

where N_f is the number of cycles to failure in the test; N_{f_o}, the number of cycles to failure in a comparable no hold time fatigue test; Σt_i, the accummulated hold time; t_{f_o}, the time to rupture of a creep test; B, a constant.

Spera (15) presented, in another mode, a method for analyzing thermal fatigue on the assumption that thermal fatigue is a combination of low-cycle fatigue and cyclic creep rupture. The damage per cycle, $1/N_t$, is the sum of the low-cycle fatigue damage per cycle, $1/N_f$, and the creep damage per cycle, $1/N_c$. A linear fatigue-creep interaction is assumed.

$$\frac{1}{N_t} = \frac{1}{N_f} + \frac{1}{N_c}$$

or

$$N_t = (\phi_f + \phi_c)^{-1} \qquad (4)$$

where N is cycles to failure; ϕ, damage per cycle, and the subscripts t, f, c denote thermal fatigue, low-cycle fatigue and cyclic creep, respectively. The fatigue damage, $\phi_f = 1/N_f$, was determined with Manson's universal slope equation (16),

$$\Delta\varepsilon = \frac{3.5}{E}\sigma_u \cdot \phi_f^{0.12} + D^{0.16} \cdot \phi_f^{0.6} \qquad (5)$$

where $\phi_f = 1/N_f$,

$\Delta\varepsilon$ = total strain range,

σ_u = ultimate tensile strength,

E = Young's modulus,

D = tensile ductility.

For the sake of being conservative, the tensile properties are evaluated at the maximum temperature of the cycle which gives the minimum life. The cyclic creep damage ϕ_c is calculated from conventional creep-rupture data,

$$\phi_c = \frac{1}{N_c} = \int_0^{\Delta t} \frac{dt}{k \cdot t_r(|S|,T)} \qquad (6)$$

where t = elapsed time,

Δt = time per cycle,

t_r = conventional creep-rupture life,

$|S|$ = absolute value of instantaneous stress,

T = instantaneous temperature,

k = 1, for uncoated alloy.

Manson and his coworkers have used a linear damage rule (17), and later an interaction damage rule (18) to successfully predict the failure lives of AISI 316 stainless steel and $2\frac{1}{4}$Cr-1Mo steel at elevated temperature in their "strainrange partitioning approach" which will be dis-

cussed in detail later.

Although in many cases the damage summation method gave a good correlation with experimental results, in some applications this rule would give under-estimated or over-estimated design guideline. Causion must be used in applying this damage rule to actual design situations.

B. FREQUENCY MODIFICATION APPROACH:

A frequency factor to modify the room temperature fatigue equation in order to predict the high temperature fatigue behavior was introduced by Eckel (19); and it was further developed by Cole et al. (20) and most recently by Coffin (21). Eckel and Cole et al. have proposed the use of a frequency-time parameter of the form $\nu^k t$. Here ν is frequency, t the failure time, and k a material constant. Coffin has developed an approach based on the concept of the "frequency modified fatigue life." The fatigue life, N_f, in the low-temperature Coffin-Manson equation, i.e.,

$$\Delta\varepsilon_p \cdot N_f^{\beta} = C \qquad (7)$$

is substituted by the frequency modified fatigue life, $\nu^k t$ or $N_f \nu^{k-1}$ to give a relation between the plastic strainrange $\Delta\varepsilon_p$, fatigue life N_f and frequency at elevated temperature, i.e.,

$$\Delta\varepsilon_p \cdot (N_f \cdot \nu^{k-1})^{\beta} = C_2$$

or

$$\Delta\varepsilon_p = C_2 \cdot (N_f \cdot \nu^{k-1})^{-\beta} \qquad (8)$$

where β, C and C_2 are constant. The important effects of time at elevated temperature are introduced by the frequency factor of cycling. He also found that the low-temperature Basquin equation (22), a relationship between the applied plastic strain range and the resulting stress range,

i.e.,

$$\Delta\sigma = A \cdot (\Delta\varepsilon_p)^n \qquad (9)$$

can be modified by a frequency term at high temperature, i.e.,

$$\Delta\sigma = A \cdot (\Delta\varepsilon_p)^n \cdot \nu^{k_1} \qquad (10)$$

The elastic strain range, $\Delta\varepsilon_e$, can be obtained by dividing the stress range in EQ.(10) by E, the Young's modulus. Together with EQ.(8), one obtains

$$\Delta\varepsilon_e = \frac{\Delta\sigma}{E} = \frac{A \cdot C_2^n}{E} \cdot N_f^{-n\beta} \cdot \nu^{k_1+(1-k)\beta n} \qquad (11)$$

The relation between the total strain range, $\Delta\varepsilon$, and N_f can be found by summing EQ.(8) and EQ.(11)

$$\Delta\varepsilon = \Delta\varepsilon_e + \Delta\varepsilon_p = \frac{A \cdot C_2^n}{E} \cdot N_f^{-n\beta} \cdot \nu^{k_1+(1-k)\beta n} + C_2 \cdot N_f^{-\beta} \cdot \nu^{(1-k)\beta} \qquad (12)$$

EQ.(12) is a generallized fatigue life prediction equation applicable to both low and high temperatures. At high temperature a set of constants A, C_2, n, β, k and k_1, must be determined for each temperature. At low temperature EQ.(12) can be converted to Manson's "universal slope equation", EQ.(5),

$$\Delta\varepsilon = \frac{3.5}{E}\sigma_u \cdot N_f^{-0.12} + D^{0.6} \cdot N_f^{-0.6}$$

by assuming no frequency effects at low temperature, i.e., k = 1 and $k_1 = 0$; and letting $\beta = 0.6$, n = 0.2, $C_2 = D^{0.6}$, and $A = 3.5\sigma_u/D^{0.12}$. EQ.(12) is useful for evaluating the low-cycle fatigue behavior of mate-

rial at high temperature. Each of the constants is directly or indirectly correlated with the better known physical properties, and the time-dependent effects are introduced by the quantities k and k_1. k modifies the plastic strain range at a given frequency and hence reflects a time-dependent ductility change, and k_1 modifies the stress range and hence is related to the time-dependent strength of material. For a specific material and temperature, a minimum of nine fatigue tests, three plastic strain ranges and three frequencies for each plastic strain range, are required to determine C_2, k and β, while A, n and k_1 can be determined from an additional specimen.

Coffin has also pointed out the possible application of this approach to hold time test results by assuming that loading wave form does not influence the fatigue result, hold time results could be predicted from ramp loading tests. Thus, if τ_c is the period of the ramp type of loading, then

$$\nu = \frac{1}{\tau_c} = \frac{1}{\tau_c' + \tau_H} \qquad (13)$$

where τ_c' is the time of strain reversal and τ_H is the hold time for each cycle.

Time-dependent effects at elevated temperature may be creep or oxidation, or both. An increase in frequency can reduce the inelastic strain per cycle by excluding time-dependent creep deformation or reduce the time available for surface-environment interaction in each cycle. Either of these two effects increases the fatigue life, but Coffin in his analysis of test results emphasizes that the environmental effect is dominant. In his tests of A286 at 1100°F and Cast Udimet 500 at 1500°F,

he found that the strong frequency effects found in air disappeared when experiments were conducted in a vacuum of 10^{-8} torr. (23) He also observed that the mode of fracture in vacuum was transgranular in contrast to the the intergranular fracture found in air. Thus, he concluded that the degradation in fatigue life found in air at elevated temperature with decreasing frequency is a result of the environment. This finding leads Coffin to emphasize that the role of the environment is dominant in elevated temperature fatigue.

C. STRAINRANGE PARTITIONING APPROACH:

Manson, Halford and Hirschberg (17,18,24) have proposed a life-prediction method, known as the "strainrange partitioning approach," which is capable of characterizing the interaction of low-cycle fatigue and creep. This method is based on the idea that cyclic inelastic strains can be separated into four possible components, i.e., $\Delta\varepsilon_{pp}$, $\Delta\varepsilon_{pc}$, $\Delta\varepsilon_{cp}$ and $\Delta\varepsilon_{cc}$. Each type of these components has a different relation to failure life. Once a given imposed inelastic strainrange is partitioned into its possible components, failure life can be determined according to an interaction damage rule. (A linear damage rule was used, when this approach was first proposed.)

Inelastic strain at elevated temperature is imposed of two different types of strain: cyclic plastic deformation and creep deformation. Cyclic plastic deformation takes place in slip bands which are distributed throughout the grains and therefore causes transgranular cracking; while the creep deformation is caused by diffusion controlled mechanisms and grain boundary sliding and migration often take place; and creep often causes intergranular cracking. Because of the basic differences in the mechanisms and the damage processes between the time-independent cyclic

plastic deformation and the time-depdndent creep deformation lead to the concept of this approach. An important feature of this approach is that a tensile component of strain must be balanced by a compressive component to close the hysteresis loop during a cycle of completely reversed straining. Any one cycle of a completely reversed inelastic strain can be partitioned into following strainrange components, as shown in Figure 1:

(a) $\Delta\varepsilon_{pp}$ – completely reversed cyclic plasticity;

(b) $\Delta\varepsilon_{pc}$ – tensile cyclic plasticity reversed by compressive creep;

$\Delta\varepsilon_{cp}$ – tensile creep reversed by compressive cyclic plasticity;

(c) $\Delta\varepsilon_{cc}$ – completely reversed creep.

Following the notation by Manson et al. (17), the first letter of the subscript (c for creep and p for cyclic plastic strain) refers to the type of strain imposed in the tensile portion of the cycle, and the second letter refers to the type of strain imposed during the compressive portion of the cycle.

Manson et al. (17) assumed that a unique relation exists between cyclic life N_{ij} and strain range $\Delta\varepsilon_{ij}$ for each of the strain components,

$$\Delta\varepsilon_{ij} = C_{ij} \cdot N_{ij}^{S_{ij}} \quad , \qquad ij = \begin{matrix} pp \\ pc \\ cp \\ cc \end{matrix} \qquad (14)$$

which is of the same form as the Manson-Coffin equation; and that the fraction of damage at failure due to each components is taken as the cycle ratio: N_f/N_{pp}, N_f/N_{pc}, N_f/N_{cp} and N_f/N_{cc}, and the damage summation equals to unity when the life is used up, i.e., linear damage rule,

$$\frac{1}{N_{pp}} + \frac{1}{N_{pc}} + \frac{1}{N_{cp}} + \frac{1}{N_{cc}} = \frac{1}{N_f} \qquad (15)$$

where N_{ij} is the failure life due to the individual partitioned component $\Delta\varepsilon_{ij}$, (ij = pp, pc, cp and cc), N_f is the predicted failure life of the imposed strainrange.

Manson (18) later proposed a "tentative universalized life relationship" for each of the four components. The normalization of the strainrange component by dividing $\Delta\varepsilon_{ij}$ by its corresponding ductility (plastic ductility D_p if the deformation imposed by the tensile half of the cycle is cyclic plasticity, creep ductility D_c if it is creep deformation) leads to a universalized equation for cyclic life associated with each of the strainrange components, analogous to the universal slopes equation. When the ratio of $\Delta\varepsilon_{ij}/D$ is plotted against the life N_{ij} in the log-log plots for a number of materials, as illustrated in Figure 2, the following empirical relations were obtained.

$$\begin{aligned} \Delta\varepsilon_{pp}/D_p &= 0.75\ N_{pp}^{-0.6} \\ \Delta\varepsilon_{pc}/D_p &= 1.25\ N_{pc}^{-0.8} \\ \Delta\varepsilon_{cp}/D_c &= 0.75\ N_{cp}^{-0.8} \\ \Delta\varepsilon_{cc}/D_c &= 0.25\ N_{cc}^{-0.8} \end{aligned} \qquad (16)$$

In Ref.(18) Manson also proppsed an "interaction damage rule" to substitute the "linear damage rule" in the life-determination, as illustrated in Figure 3,

$$\frac{F_{pp}}{N_{pp}} + \frac{F_{pc}}{N_{pc}} + \frac{F_{cp}}{N_{cp}} + \frac{F_{cc}}{N_{cc}} = \frac{1}{N_f} \qquad (17)$$

where F_{ij} is the fraction of the total inelastic strainrange that is due to $\Delta\varepsilon_{ij}$, and N_{ij} is the life obtained from the life-relationship by considering the entire inelastic strainrange to be $\Delta\varepsilon_{ij}$.

Having discussed the life-relationships and the damage rule, now the basic problem is how to partition the total imposed strainrange into its three components (although there are four possible components, $\Delta\varepsilon_{pc}$ and $\Delta\varepsilon_{cp}$ cannot exist simultaneously). The detail of the experimental procedures of how to partition the imposed strainrange was given in Refs. 17, 18, 24 and 25. A brief summary is given in Figures 4 and 5. The partitioned strainrange $\Delta\varepsilon_{pp(a)}$ is $\Delta\varepsilon_{pp}$, if the loading rate is high enough to preclude creep deformation. However, if the loading rate is not high enough, a considerable amount of creep deformation may be imposed in this apparent cyclic plasticity $\Delta\varepsilon_{pp(a)}$. In this case, $\Delta\varepsilon_{pp(a)}$ is the sum of cyclic plasticity and creep deformation. In order to determine the amount of creep deformation imposed in the strain reversal portion of the cycle, $\Delta\varepsilon'_{cc}$, a supplementary fast cycling test should be performed, as shown in Figures 4(a) and 5(a). The hysteresis loop is first established after applying cycles of loading at the frequency (neglecting hold time) involved, then develope an inner loop by rapid cycling (with a frequency high enough to preclude appreciable creep) between the stress extremes developed in the previous step. $\Delta\varepsilon_{pp}$ is determined from the rapid cycling, and the $\Delta\varepsilon'_{cc}$ the difference between $\Delta\varepsilon_{pp(a)}$ and $\Delta\varepsilon_{pp}$. The fraction of strain reversal, which is associated with $\Delta\varepsilon'_{cc}$, F'_{cc}, is then

$$F'_{cc} = \frac{\Delta\varepsilon'_{cc}}{\Delta\varepsilon_{pp(a)}} = \frac{\Delta\varepsilon'_{cc}}{\Delta\varepsilon_{pp} + \Delta\varepsilon'_{cc}} \qquad (18)$$

The procedure of how to partition strainrange components are illustrated in Figures 4 and 5. The fractions of $\Delta\varepsilon_{pp}$, $\Delta\varepsilon_{pc}$, $\Delta\varepsilon_{cp}$ and $\Delta\varepsilon_{cc}$ of the total inelastic strainrange are also shown in the figures. It should be noted that the fraction of total inelastic strainrange associated with cc type of strainrange is the sum of those associated with $\Delta\varepsilon'_{cc}$ and $\Delta\varepsilon_{cc}$, i.e.,

$$F_{cc} = F'_{cc} \frac{\Delta\varepsilon_{pp(a)}}{\Delta\varepsilon_{in}} + \frac{\Delta\varepsilon_{cc}}{\Delta\varepsilon_{in}} \qquad (19)$$

and that associated with $\Delta\varepsilon_{pp}$ component is

$$F_{pp} = (1 - F'_{cc}) \frac{\Delta\varepsilon_{pp(a)}}{\Delta\varepsilon_{in}} \qquad (20)$$

It will be also noted that in Figure 4(d) and 5(d), as defined $\Delta\varepsilon_{cc}$ is the smaller of the two creep strains, FB; and $\Delta\varepsilon_{pp(a)}$ is the smaller of the two plastic strains, HB. Since part of the tensile plasticity and part of the compressive creep are left, the $\Delta\varepsilon_{pc}$ component is given by the difference between the total inelastic strainrange and $(\Delta\varepsilon_{pp(a)} + \Delta\varepsilon_{cc})$.

The advantages of this approach are manyfold: establishing bounds on life; simplifying temperature effects; and successfully accounting for the effects of frequency, hold time, creep and stress relaxation, and environment.

(a). ESTABLISHING BOUNDS ON LIFE:

The concept of bounds on life has been first proposed by Manson in his "10-percent rule" (26):

$$\Delta\varepsilon = \frac{3.5\ \sigma_u}{E} N_f^{-0.12} + D^{0.6} N_f^{-0.6}$$

$$N_f' = 0.10\ N_f \qquad (21)$$

in which the life at elevated temperature N_f' is assumed to be reduced to 10 % of its room-temperature value to account for creep or stress relaxation; and it was again proposed in his " combination of fatigue and creep effect" (27):

$$(\text{ creep-rupture damage }) + (\text{ fatigue damage }) = 1$$

$$\left(\frac{t'}{t_r}\right) + \left(\frac{N_f'}{N_f}\right) = 1$$

where $t' = (k/F)\ N_f'$

$$t_r = A\ (\sigma_r/1.75\sigma_u)^{1/m} = A\ (N_f)^{-0.12/m}$$

hence:

$$\frac{k\ N_f'}{A\ F\ (N_f)^{-0.12/m}} + \left(\frac{N_f'}{N_f}\right) = 1$$

or

$$N_f' = \frac{N_f}{1 + k/AF(N_f)^{(m + 0.12)/m}} \qquad (22)$$

where N_f' = number of cycles to failure under combined fatigue and creep,

N_f = number of cycles to failure in fatigue based on method of universal slopes,

k = constant,

A and m = conatants given by the representation of creep-rupture curve by $\sigma_r = 1.75\sigma_u\ (t_r/A)^m$, where σ_r is the steadily applied stress, and σ_u is the ultimate tensile strength,

F = frequency of cycling.

The Manson-Halford estimation on life-bounds (28) is then summarized as follow:

(1). Determine the lower bound of life N_f', using either EQ.(21) or EQ.(22), whichever is lower.

(2). For the average life, use twice the lower bound life.

(3). For the upper life, use ten times the lower bound life.

In this method, estimates of average life and the upper and lower bounds are provided for a given set of test conditions.

An important use of the strainrange partitioning approach is very similar to this. Since the imposed inelastic strainrange can be partitioned into four possible components, the life-relationship of the most damaging component gives the lowest bound on life, and that of the least damaging one gives the upper bound on life. The concept of life-bounds simplifies the complexity of the analysis and provides a conservative estimate of failure life. Even if only the total inelastic strainrange is known and no further strainrange partitioning analysis is made, the lowest bound on life gives a conservative life-estimate regarding all the imposed inelastic strainrange as the most damaging component. If it is known that certain components are present and others are excluded, only the life-relationships associated with those components present are used for the estimate of lowest bound. However, if a complete analysis is made, knowing the magnitude of each possible component, an accurate life-estimate can be achieved.

(b). SIMPLIFYING TEMPERATURE EFFECTS:

Halford et al. (29) proposed that the strainrange-life relationship for each of the four components are independent of temperature. However, temperature will affect the partitioning of the total inelastic strain-

range into its components. Under the same loading conditions except at different temperatures, a given imposed inelastic strainrange will be partitioned into different manner depending on the test temperature, hence the fatigue life will be different at different temperature. However, if a given imposed inelastic strain is partitioned into the same manner at different temperatures, the fatigue life will be the same in spite of different test temperature. Conclusively, the fatigue life is dependent on the manner of strainrange partitioning which is dependent on the temperature; while the strainrange-life relationship of each type of strainrange is independent of temperature. Once the imposed strain is partitioned into its components, the failure life can be estimated without regarding for temperature.

(c). EXPLANATION OF FREQUENCY EFFECTS:

The hysteresis loops in Figure 6 are developed by the same procedures as discussed before but the total inelastic strain is kept constant for each test. Limiting values of failure life exist at both extremes of frequencies, low and high. At the low frequency extreme all the applied strain tends to be $\Delta\varepsilon_{cc}$. Further decrease in frequency does not increase the amount of $\Delta\varepsilon_{cc}$, so that failure life levels off at N_{cc} for the applied strainrange. Similarly, at the highest frequency extreme, life levels off at N_{pp} for the applied strainrange.

(d). EXPLANATION OF HOLD-TIME AND CREEP OR RELAXATION EFFECTS:

Creep or stress relaxation occurs during the tensile or compressive stress or strain hold period. This creep strain may later be reversed by cyclic plastic deformation, thus $\Delta\varepsilon_{cp}$ or $\Delta\varepsilon_{pc}$ components may developed; or by creep deformation, then $\Delta\varepsilon_{cc}$ may occur. Increasing hold times increases the creep component, i.e., $\Delta\varepsilon_{cp}$, $\Delta\varepsilon_{pc}$, or $\Delta\varepsilon_{cc}$ depending on where

the hold times are introduced, and then reduces the failure life.

(e). EXPLANATION OF ENVIRONMENT EFFECTS:

The environmental effect (most possibly, oxidation) is an additional time-dependent variable in high temperature fatigue. When frequency is lowered or hold periods are introduced, there is more time not only for creep but also for oxidation or other surface reaction. There exists an argument regarding the relative role of creep and environment on high-temperature fatigue life. However, it should be noted that even if the environmental effect is dominant, provided that the basic strain-life relationships are obtained under the same environment as that it is to be applied, the strainrange partitioning approach is still valid.

HIGH-TEMPERATURE FATIGUE CRACK GROWTH:

The principles of linear-elastic fracture mechanics have been successfully applied in characterizing the propagation of fatigue cracks in the austenitic stainless steel at elevated temperature by Brothers (30), James (31), and Shahinian (32). As long as the average stresses in the net section remain generally elastic, the crack growth rate (da/dN) is governed by the crack tip stress intensity factor range (Δ K). At room temperature, there is no significant effect of frequency and cyclic loading wave form on fatigue crack growth rate. However, the creep effect, the environmental effect (most possibly, oxidation), as well as the mechanical properties of materials themselves strongly enhance the crack growth rate at elevated temperature. This means that the effects of temperature, frequency, hold time, loading wave form, and environment on fatigue crack growth rate should be considered at high temperature.

A. TEMPERATURE EFFECTS:

An increase in temperature generally increases crack growth rate for

a given ΔK and reduces the threshold ΔK for crack growth. When the data are plotted as log(da/dN) versus log(ΔK) for each test temperature, slope transitions occur but do not exhibit a consistent trend with temperature. Shahinian et al. (33) showed that normalizing ΔK by dividing by the square of Young's modulus for the various temperatures tends to agglomerate the data to a single curve. More recently, Speidel (2) indicated that the normalization of ΔK with Young's modulus tends to unify fatigue crack growth rate data in vacuum, and that the effect of temperature on cycle-dependent fatigue crack growth in vacuum is resulted from the temperature dependence of the Young's modulus. He then assumed that fatigue crack growth in air is about three times faster than in vacuum, even in high temperature, provided that the cycling frequency is high enough to preclude the time-dependent effects. His prediction based on the modulus correction agreed very well with experimental data. Then, he concluded that the increase of cycle-dependent fatigue crack growth rate with increasing temperature is correlated with the corresponding decrease of Young's modulus.

Wei (34) in his investigation of crack growth rate in 7075-T651 aluminum alloy reported that crack growth rate data fitted the Arrhenius type relationship over a temperature range of 70 to 212°F. He suggested that an Arrhenius type equation may be employed,

$$\frac{da}{dN} = A \cdot f(\Delta K) \cdot \exp[\frac{-u(\Delta K)}{kT}] \qquad (23)$$

Where A is a constant, $f(\Delta K)$ crack driving force, $u(\Delta K)$ apparent activation energy, k Boltzmann's constant, and T absolute temperature.

More recently, Jeglic et al. (35) have studied the fatigue crack

growth in an Al-2.6Mg alloy between room temperature and 572°F, and shown that the crack propagation rate coule be described in terms of

$$\frac{da}{dN} = A(\Delta K) \cdot \exp\left(\frac{-Q(\Delta K)}{RT}\right) \qquad (24)$$

where $A(\Delta K) = C_2 K^{-2}$ is a coefficient including a constant driving force, $Q(\Delta K) = Q_o - C_1 \log \Delta K$ the apparent activation energy, Q_o the basic activation energy, and R the gas constant.

James et al. (31) and Shahinian et al. (32) have shown that the crack growth rate data of AISI 304 stainless steel over the range of 75 to 1200°F and of AISI 316 stainless steel over the range of 70 to 1100°F, respectively, do not conform to a single Arrhenius type relationship. The data, when plotted in an Arrhenius fashion of log (da/dN) versus 1/T, was non-linear for any particular value of ΔK. Since fatigue crack growth at elavated temperature is obviously a thermally-activated process, they concluded that rather than a single thermally-activated process, more than one process is dominant in fatigue cracking over the entire temperature range and a more complete definition of the pre-exponential term, A, is needed.

B. FREQUENCY EFFECTS:

James (36) found that, in the plot of log (da/dN) versus log (ΔK) for various frequencies, there exists a critical value of ΔK, beyond which the crack growth rate increases with decreasing frequency, while below which there shows a frequency independency on crack growth.

Ohmura et al. (37) indicated further that, as shown in Figure 7, in many cases a critical frequency is observed, below which the crack growth rate is inversely proportional to the frequency. In the low fre-

quency range, cracking is generally intergranular; while in the high frequency range, the crack path is transgranular and the effect of frequency on crack growth is negligible. Around the critical frequency there is a transition frequency range with mixed fracture mode and a weak frequency-dependence. Spiedel (2) summarily illustrated schematically the frequency dependence of crack growth rate, as shown in Figure 8, which is in turn influenced by the cyclic stress intensity factor range.

Solomon and Coffin (3) in their high-temperature low-cycle fatigue crack growth investigations in air and in vacuum also showed a very similar results as Ohmura's. Figure 9 shows that at high frequencies there is a frequency-independent and purely cycle-dependent transgranular crack growth rate with a slope of 0, and at low frequencies a purely time-dependent intergranular crack growth rate with a slope of -1 in the plot of log (da/dN) versus log ν. In the curve for the tests in air there is an extended transition region in which the crack growth is of mixed fracture mode and is weak frequency dependent. In the curve for the vacuum test there is a linear damage rule region in which the sum of the time and cycle fraction is approximately unity.

C. HOLD TIME EFFECTS:

Speidel (2) indicated that there are two different mechanisms by which hold times can affect the over-all crack growth. First, under some circumstances, if the time-dependent creep crack growth is significantly faster than the cycle-dependent fatigue crack growth, crack growth rate may be directly proportional to the length of the hold period. Secondly, if there is no significant creep crack growth during the hold period, hold time may still affect the overall crack growth by increasing time for the reaction of environment with newly formed crack surface created during

the opening half cycle.

Generally, the longer the hold time the faster will be the crack growth rate. Mowbray et al. (38) in their measurements of crack growth in Rene 77 and FSX 414 alloys, found that the crack growth rate increases with increasing the hold period until a hold period of 16 mins.; for the hold period longer than 16 mins. the crack growth rate decreases in stead of increasing. Further they found that a new metallurgical phase precipitated, which hardened the material and reduced the crack growth rate, as the hold time exceeds 16 mins. Therefore, we must also concern with the metallurgical instability in the hold time effects on fatigue crack growth at elevated temperature.

D. ENVIRONMENT EFFECTS:

Although there is still an argument that whether the environmental effects or the creep effects decisively influence the fatigue crack growth at elevated temperature, it is believed that both of them strongly affect the crack growth. Both of environmental and creep effects are time-dependent, it is difficult to distinguish between them in an actual performance of a machine component. Nevertheless, since the most possible concern of environmental effects at elevated temperature is the oxidation, strain-enhanced oxide formation near a crack tip can either advantageously or deleteriously modify crack propagation. (5,39) Vacuum rewelding upon crack closure, oxide bridging and load bearing, and oxide filling preventing compression resharpening may decrease the crack growth rate. Oxide wedging at crack tip and oxide formation and subsequent rupturing may increase the crack growth rate.

Although the temperature- and time-dependent factors which influence the fatigue crack growth rate at elevated temperature, have been dis-

cussed individually, it is also interesting to be concerned with that when these factors exist concurrently. Popp and Coles (40) used the Larson-Miller parameter to describe time-temperature effects on cyclic crack growth rate at a particular stress intensity range, Figure A10. The time-temperature parameter, $P = (T + 460)\cdot(C + \log t_h)$, where T is temperature, ^{o}F; t_h, the hold time per cycle, hrs.; C, a material constant, reasonably described crack growth rate for temperature raging from 70 to $1200^{o}F$ and peak stress hold time from 0 to 2 hrs.

Carden (41) on his analysis of the data of AISI 304 stainless steel provided a parametric relationship relating the crack growth rate to the effects of stress ratio, K_{max}, K_{th}, frequency, and temperature.

$$\frac{da}{dN} = P(K_{max}, R, \nu, T)$$

and

$$P = A_1(\nu, T) \cdot (K_e^2 - K_{e_{th}}^2)^m \qquad (25)$$

where $A_1(\nu, T) = [A_{11}(T)\cdot(1/\nu)^k + C_{11}(T)\cdot(1/\nu)]_T = \text{constant}$

$$A_{11}(T) = A_{1101} \exp(-\Delta H_1/RT) + A_{1102} \exp(-\Delta H_2/RT)$$

and $$K_e^2 - K_{e_{th}}^2 = (K_{max}^2 - K_{th}^2) \cdot (1 - R)^{2n}$$

i.e. $$P = \{[A_{1101} \exp(-\Delta H_1/RT) + A_{1102} \exp(-\Delta H_2/RT)] \cdot (1/\nu)^k + C_{1101} \exp(-\Delta H_3/RT) \cdot (1/\nu)\}[(K_{max}^2 - K_{th}^2) \cdot (1-R)^{2n}]^m \qquad (26)$$

where T = temperature,

ν = frequency,

K_{max} = the maximum stress intensity of the cycle,

K_{th} = the threshold value of stress intensity factor,

ΔH_1 = the activation energy for high temperature range where creep, self-diffusion or similar process are active,

ΔH_2 = the activation energy for low temperature range where there is a slight thermal dependency to the yield strength and Young's modulus,

R = the stress ratio,

A, C, k and m = material-environment combination constants.

The derivation of EQ.(26) is also illustrated in Figure 11 . Carden treated all of the frequency and temperature effects on crack growth rate in the coefficient A_1. He assumed that these effects can be summed up by those in high frequency cycle-dominant region, A_{11} term, and those in low frequency creep-dominant region, C_{11} term. He also assumed that there are multiple thermally-activated processes governing A_{11}, which can be separated into high and low temperature dominant ones, A_{1101} and A_{1102}, respectively, and a single thermally-activated process governs C_{11}.

REFERENCES

1. Wells, C. H., Sullivan, C. P., and Gell, M., "Mechanisms of Fatigue in the Creep Range", Metal Fatigue Damage-Mechanism, Detection, Avoidance, and Repair, ASTM STP 495, American Society for Testing and Materials, 1971, pp. 61-122.

2. Speidel, M. O., "Fatigue Crack Growth at High Temperature", in High-Temperature Materials in Gas Turbines, P. R. Sahm and M. O. Speidel ed., Elsevier Scientific Publishing Co., Amsterdam, Netherland, 1974, pp. 207-255.

3. Solomon, H. D., and Coffin, L. F., Jr., "Effects of Frequence and Environment on Fatigue Crack Growth in A286 at 1100°F", Fatigue at Elevated Temperature, ASTM STP 520, American Society for Testing and Materials, 1973, pp. 112-122.

4. Krempl, E., and Wundt, M., "Hold-Time Effects in High Temperature Low-Cycle Fatigue", ASTM STP 489, American Society for Testing and Materials, 1971.

5. Gell, M., Leverant, G. R. and Wells, C. H., "The Fatigue Strength of Nickel-Base Superalloys," Achievement of High Fatigue Resistance in Metals and Alloys, ASTM STP 467, American Society for Testing and Materials, 1970, pp. 113-153.

6. Feltner, C. E. and Mitchell, M. R., "Basic Research on the Cyclic Deformation and Fracture Behavior of Materials," Manual on Low Cycle Fatigue Testing, ASTM STP 465, American Society for Testing and Materials, 1969, pp. 27-66.

7. Miner, M. A., "Cumulative Damage in Fatigue", Transaction of ASME, Vol. 67, A159, 1945.

8. Robinson, E. L., "Effect of Temperature Variation on the Long-time Rupture Strength of Steels", Transaction of ASME, Vol. 74, No. 5, 1952, pp. 777-781.

9. Taira, S., "Lifetime of Structures Subjected to Varying Load and Temperature", Creep in Structure, N. J. Hoff, ed., Academic Press, New York, 1962, pp. 96-124.

10. "Code Case 1592: Nuclear Vessels in High Temperature Service", Section III ASME Boiler and Pressure Vessel Code, 1974.

11. Gittus, J. H., "Implication of Some Data on Relaxation Creep in Nimonic 80A", Philosophical Magazine, Vol. 9, 1964, pp. 749-753.

12. Campbell, R. D., "Creep/Fatigue Interaction Correlation for 304 Stainless Steel Subjected to Strain-Controlled Cycling with Hold Time at Peak Strain", Journal of Engineering for Industry, Transactions, ASME, Vol. 93, No. 4, Nov. 1971, pp. 887-892.

13. Jaske, C. E., Mindlin, H., and Perrin, J. S., "Combined Low-Cycle Fatigue and Stress Relaxation of Alloy 800 and Type 304 Stainless Steel at Elevated Temperature", Fatigue at Elevated Temperature, ASTM STP 520, American Society for Testing and Materials, 1973, pp. 365-376.

14. Lagneborg, R., and Attermo, R., "The Effect of Combined Low-Cycle Fatigue and Creep on the Life of Austenitic Stainless Steel", Metallurgical Transactions, Vol. 2, No. 7, July 1971, pp. 1821-1827.

15. Spera, D. A., "Comparison of Experimental and Theoretical Thermal Fatigue Lives for Five Nickel-Base Alloys", Fatigue at Elevated Temperature, ASTM STP 520, 1973, pp. 648-657.

16. Manson, S. S., "Fatigue: A Complex Subject-Some Simple Approximations", Experimental Mechanics, Vol. 5, No. 7, July 1965, pp. 193-226.

17. Manson, S. S., Halford, G. R., and Hirschberg, M. H., "Creep-Fatigue Analysis by Strainrange Partitioning", Symposium on Design for Elevated Temperature Environment, American Society of Mechanical Engineering, New York, 1971, pp. 12-24.

18. Manson, S. S., "The Challenge to Unify Treatment of High Temperature Fatigue - A Partisan Proposal Based on Strainrange Partitioning", Fatigue at Elevated Temperature, ASTM STP 520, 1973, pp. 744-782.

19. Eckel, J. F., "The Influence of Frequency on the Repeated Bending Life of Acid Lead", Proceedings, American Society for Testing and Materials, Vol. 51, 1951, pp. 745-746.

20. Coles, A., Hill, G. J., Dawson, R. A. J., and Watson, S. J., "The High Strain Fatigue Properties of Low Alloy Creep Resisting Steels", International Conference on Thermal and High Strain Fatigue, The Metals and Metallurgy Trust, England, 1967, pp. 270-294.

21. Coffin, L. F., Jr., "The Effect of Frequency on High-Temperature Low-Cycle Fatigue", Proceedings of the Air Force Conference on Fatigue and Fracture of Aircraft Structures and Materials, AFFDL TR 70-144, 1970, pp. 301-311.

22. Basquin, O. h., "The Exponential Law of Endurance Tests," Proceedings, American Society for Testing and Materials, ASTEA, Vol. 10, 1910, pp. 625-630.

23. Coffin, L. F., Jr., "Fatigue at High Temperature", Fatigue at Elevated Temperature, ASTM STP 520, American Society for Testing and Materials, 1973, pp. 5-34.

24. Manson, S. S., Halford, G. R. and Nachligall, A. J., "Separation of the Strain Components for Use in Strainrange Partitioning", NASA TM X-71737, National Aeronautics and Space Administration, Cleveland, Ohio, 1975.

25. Leven, M. M., "The Interaction of Creep and Fatigue for a Rotor Steel", Experimental Mechanics, Vol. 13, No. 9, 1973, pp. 353-372.

26. Manson, S. S., "Interfaces Between Fatigue, Creep, and Fracture", International Journal of Fracture Mechanics, Vol. 2, No. 1, 1966, pp. 327-363.

27. Manson, S. S., and Halford, G. R., "A Method of Estimating High-Temperature, Low-Cycle Fatigue Behavior of Materials", Proceedings, International Conference on Thermal and High Strain Fatigue, Metals and Metallurgy Trust, London, England, 1967, pp. 154-170.

28. Manson, S. S., "A Simple Procedure for Estimating High Temperature Low Cycle Fatigue", Paper presented at the Spring Meeting of the SESA, held on May 16-19, 1967, in Ottawa, Ontario, Canada.

29. Halford, G. R., Hirschberg, M. H., and Manson, S. S., "Temperature Effects on the Strainrange Partitioning Approach for Creep Fatigue Analysis", Fatigue at Elevated Temperature, ASTM STP 520, 1973, pp. 658-669.

30. Brothers, A. J., "Fatigue Crack Growth in Nuclear Reactor Piping Steel", General Electric Report GEAP-5607, Mar. 1968.

31. James, L. A., and Schwenk, E. B. Jr., "Fatigue-Crack Propagation of Type 304 Stainless Steel at Elevated Temperatures", Metallurgical Transaction, Vol. 2, No. 2, 1971, pp. 491-496.

32. Shahinian, P., Smith, H. H., and Watson, H. E., "Fatigue Crack Growth in Type 316 Stainless Steel at High Temperature", Journal of Engineering for Industry, Transaction, American Society of Mechanical Engineering, Vol. 93, No. 4, 1971, pp. 976-980.

33. Shahinian, P., Watson, H. E., and Smith, H. H., "Fatigue Crack Growth in Selected Alloys for Rotor Applications", Journal of Materials, Vol. 7, No. 4, 1972, pp. 527-535.

34. Wei, R. P., "Fatigue-Crack Propagation in a High-Strength Aluminum Alloy", The International Journal of Fracture Mechanics, Vol. 4, No. 2, 1968, pp. 159-168.

35. Jeglic, F., Niessen, P., and Burns, D. J., "Temperature Dependence of Fatigue Crack Propagation in an Al-2.6Mg Alloy", Fatigue at Elevated Temperature, ASTM STP 520, American Society for Testing and Materials, 1972, pp. 139-148.

36. James, L. A., "The Effect of Frequency upon the Fatigue-Crack Growth of Type 304 Stainless Steel at 1000°F", Stress Analysis and Growth of Crack, ASTM STP 513, American Society for Testing and Materials, 1972, pp. 218-229.

37. Ohmura, T., Pelloux, R. M., and Grant, N. J., "High Temperature Fatigue Crack Growth in a Cobalt Base Superalloy", Engineering Fracture Mechanics, Vol. 5, 1973, pp. 909-922.

38. Mowbray, D. F., and Woodford, D. A., "Observations and Interpretation of Crack Propagation Under Conditions of Transient Thermal Strain", International Conference on Creep and Fatigue in Elevated Temperature Applications, Institution of Mechanical Engineering, Sheffield, U.K., 1973.

39. Cook, R. H., and Skelton, R. P., "Environment-Dependence of the Mechanical Properties of Metals at High Temperature", International Metallurgical Review, Vol. 19, 1974, pp. 199-222.

40. Popp, H. G., and Coles, A., "Subcritical Crack Growth Criteria for Inconel 718 at Elevated Temperature", Proceedings, Air Force Conference on Fatigue and Fracture of Aircraft Structures and Materials, AFFDL TR 70-144, 1970, pp. 71-86.

41. Carden, A. E., "Parametric Analysis of Fatigue Crack Growth", International Conference on Creep and Fatigue in Elevated Temperature Applications, Institution of Mechanical Engineering, Sheffield, U.K., 1973.

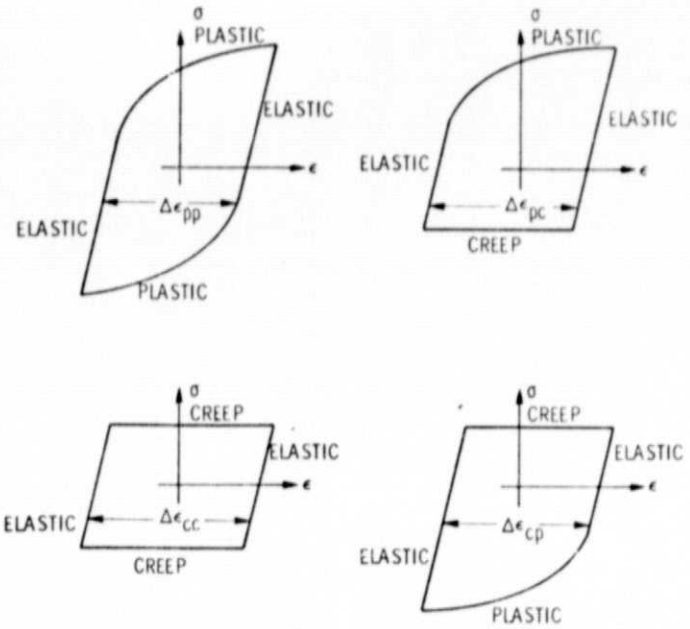

FIG. 1 IDEALIZED HYSTERESIS LOOP FOR THE FOUR BASIC TYPES OF INELASTIC STRAIN-RANGE (From Halford et al., Ref. A29).

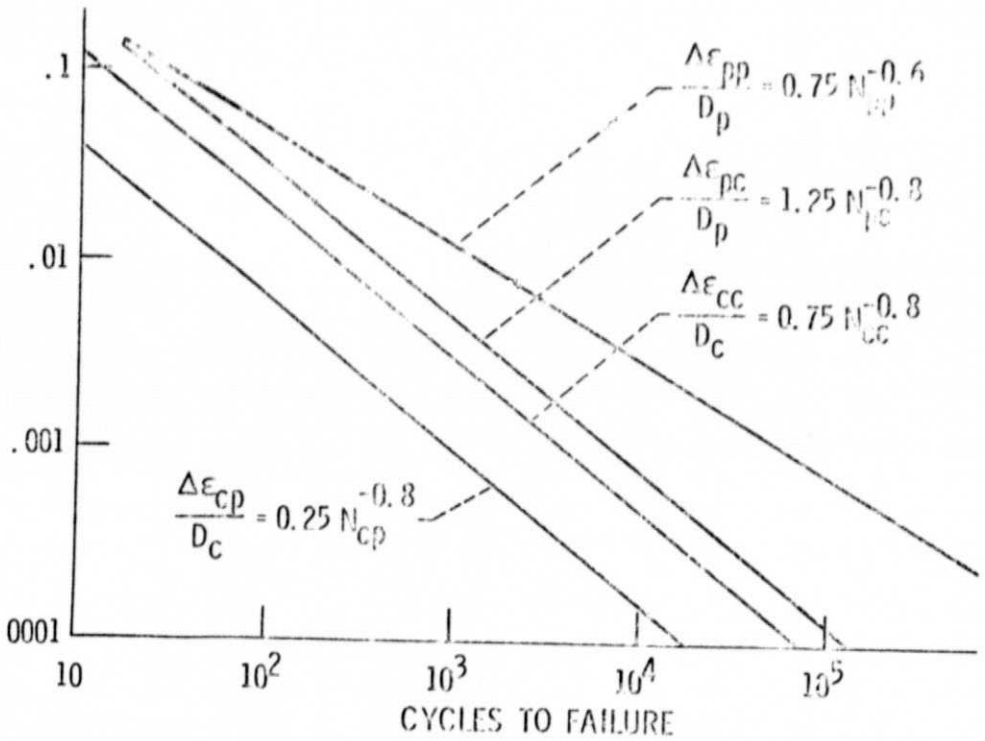

FIG. 2 TENTATIVE UNIVERSALIZED RELATIONSHIPS FOR THE FOUR STRAIN-RANGE COMPONENTS (From Manson, Ref. A18).

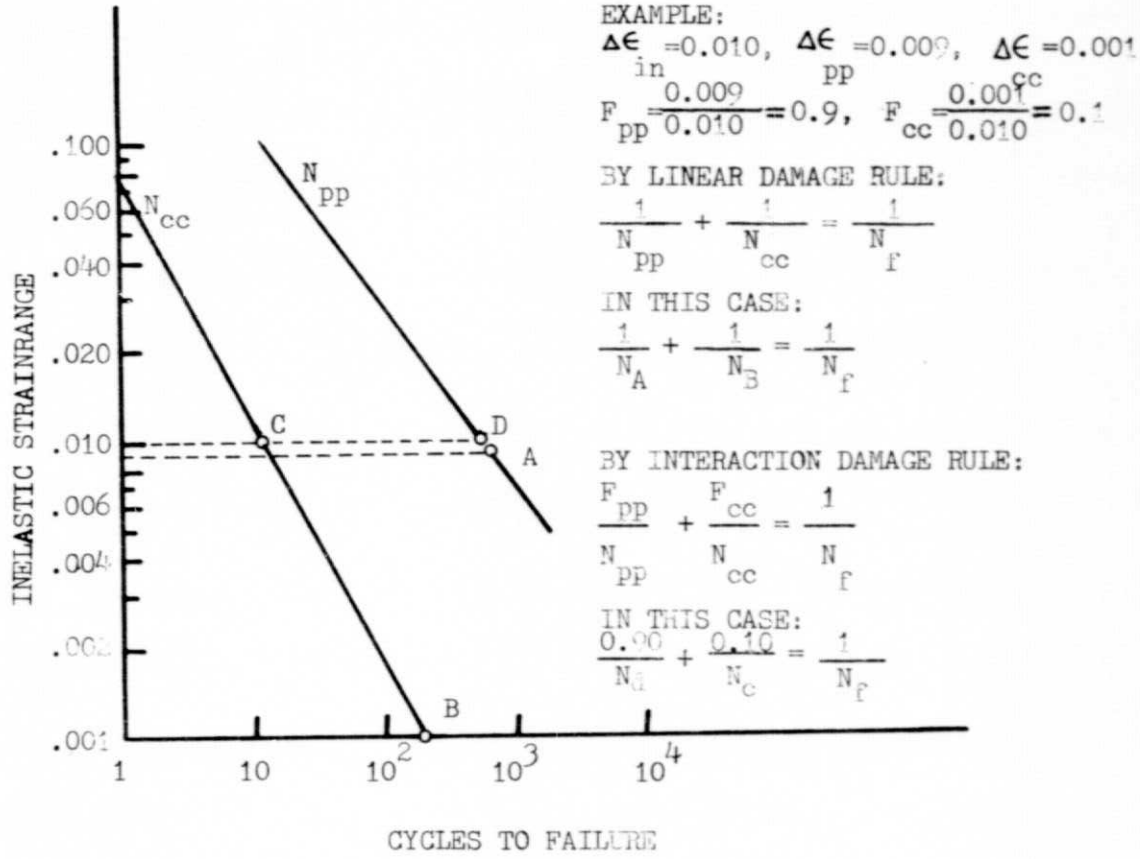

FIG. 3 LIFE-PREDICTION BY STRAINRANGE PARTITIONING APPROACH (From Manson, Ref. A18).

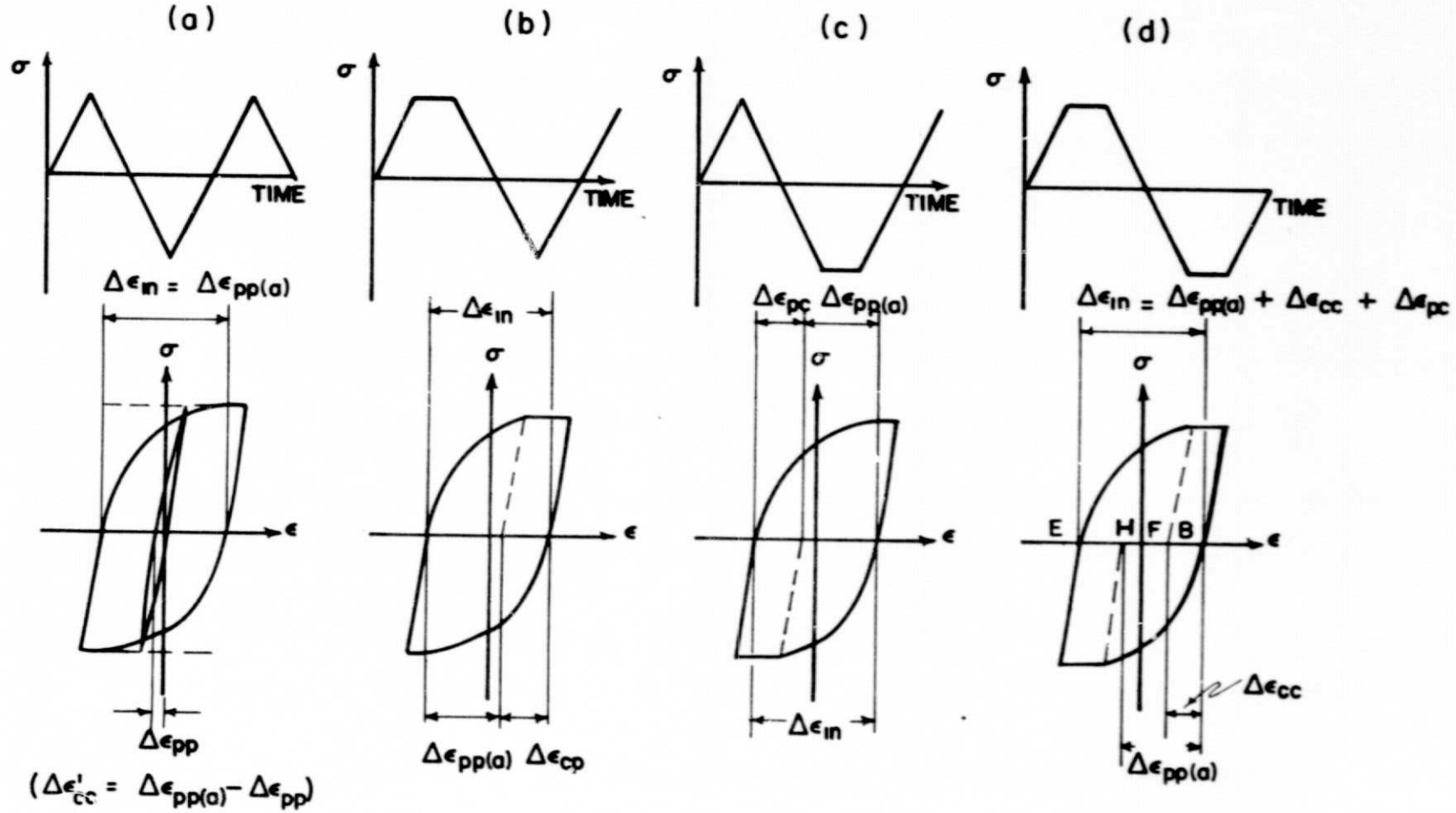

$$\begin{cases} F_{pp} = \dfrac{\Delta\epsilon_{pp}}{\Delta\epsilon_{in}} \\ F'_{cc} = \dfrac{\Delta\epsilon_{pp(a)} - \Delta\epsilon_{pp}}{\Delta\epsilon_{in}} \\ \quad = F_{cc} \end{cases}$$

$$\begin{cases} F_{pp} = (1-F'_{cc}) \dfrac{\Delta\epsilon_{pp(a)}}{\Delta\epsilon_{in}} \\ F_{cc} = F'_{cc} \dfrac{\Delta\epsilon_{pp(a)}}{\Delta\epsilon_{in}} \\ F_{cp} = \dfrac{\Delta\epsilon_{cp}}{\Delta\epsilon_{in}} \end{cases}$$

$$\begin{cases} F_{pp} = (1-F'_{cc}) \dfrac{\Delta\epsilon_{pp(a)}}{\Delta\epsilon_{in}} \\ F_{cc} = F'_{cc} \dfrac{\Delta\epsilon_{pp(a)}}{\Delta\epsilon_{in}} \\ F_{pc} = \dfrac{\Delta\epsilon_{pc}}{\Delta\epsilon_{in}} \end{cases}$$

$$\begin{cases} F_{pp} = (1-F'_{cc}) \dfrac{\Delta\epsilon_{pp(a)}}{\Delta\epsilon_{in}} \\ F_{cc} = F'_{cc} \dfrac{\Delta\epsilon_{pp(a)}}{\Delta\epsilon_{in}} + \dfrac{\Delta\epsilon_{cc}}{\Delta\epsilon_{in}} \\ F_{pc} = \dfrac{\Delta\epsilon_{in} - \Delta\epsilon_{pp(a)} - \Delta\epsilon_{cc}}{\Delta\epsilon_{in}} \end{cases}$$

FIG. 4 SEPARATION OF STRAINRANGE IN STRESS-CONTROLLED FATIGUE CYCLES.

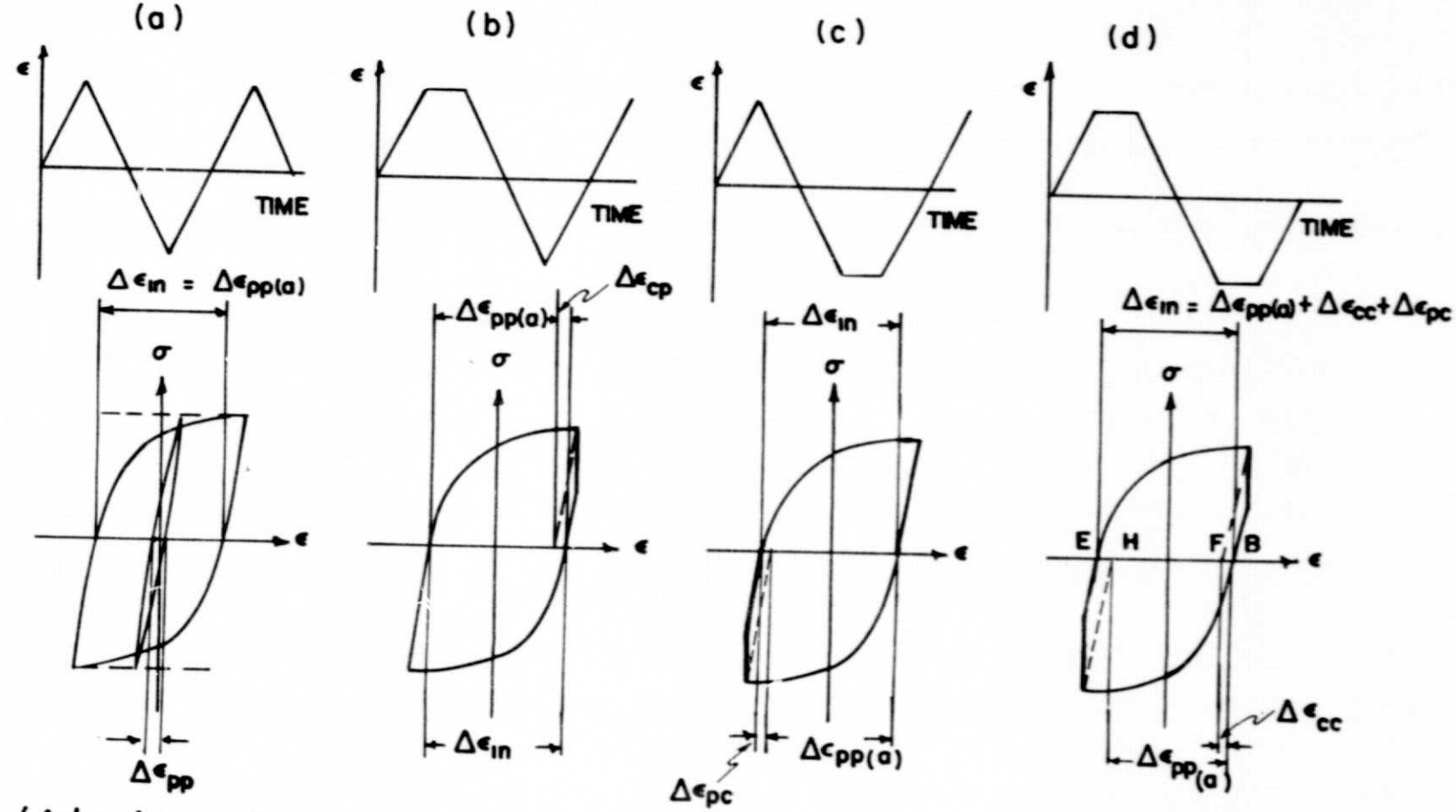

$(\Delta\epsilon_{cc} = \Delta\epsilon_{pp(a)} - \Delta\epsilon_{pp})$

$$\begin{cases} F_{pp} = \dfrac{\Delta\epsilon_{pp}}{\Delta\epsilon_{in}} \\ F'_{cc} = \dfrac{\Delta\epsilon_{pp(a)} - \Delta\epsilon_{pp}}{\Delta\epsilon_{in}} \\ \quad = F_{cc} \end{cases} \qquad \begin{cases} F_{pp} = (1 - F'_{cc}) \dfrac{\Delta\epsilon_{pp(a)}}{\Delta\epsilon_{in}} \\ F_{cc} = F'_{cc} \dfrac{\Delta\epsilon_{pp(a)}}{\Delta\epsilon_{in}} \\ F_{cp} = \dfrac{\Delta\epsilon_{cp}}{\Delta\epsilon_{in}} \end{cases} \qquad \begin{cases} F_{pp} = (1 - F'_{cc}) \dfrac{\Delta\epsilon_{pp(a)}}{\Delta\epsilon_{in}} \\ F_{cc} = F'_{cc} \dfrac{\Delta\epsilon_{pp(a)}}{\Delta\epsilon_{in}} \\ F_{pc} = \dfrac{\Delta\epsilon_{pc}}{\Delta\epsilon_{in}} \end{cases} \qquad \begin{cases} F_{pp} = (1 - F'_{cc}) \dfrac{\Delta\epsilon_{pp(a)}}{\Delta\epsilon_{in}} \\ F_{cc} = F'_{cc} \dfrac{\Delta\epsilon_{pp(a)}}{\Delta\epsilon_{in}} + \dfrac{\Delta\epsilon_{cc}}{\Delta\epsilon_{in}} \\ F_{pc} = \dfrac{\Delta\epsilon_{in} - \Delta\epsilon_{pp(a)} - \Delta\epsilon_{cc}}{\Delta\epsilon_{in}} \end{cases}$$

FIG. 5 SEPARATION OF STRAINRANGE IN STRAIN-CONTROLLED FATIGUE CYCLES.

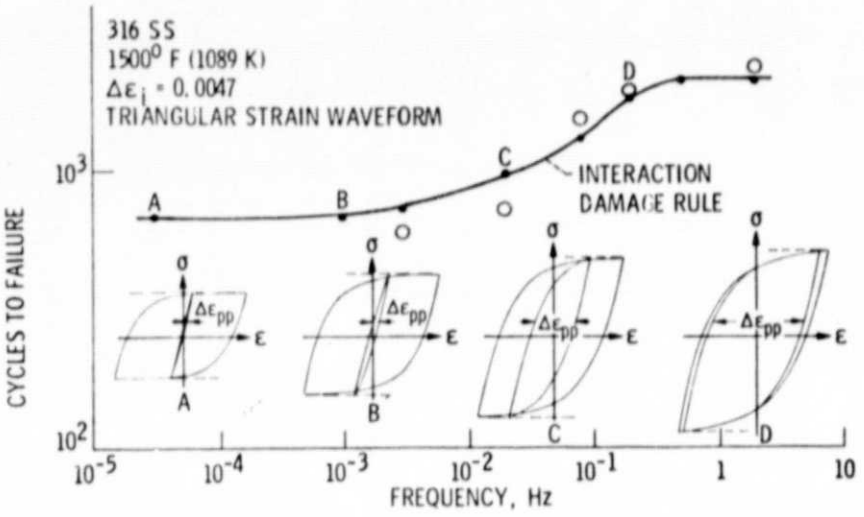

FIG. 6 EXPLANATION OF FREQUENCY EFFECTS ON FAILURE LIFE BY STRAIN-RANGE PARTITIONING APPROACH (From Manson, Ref. A18).

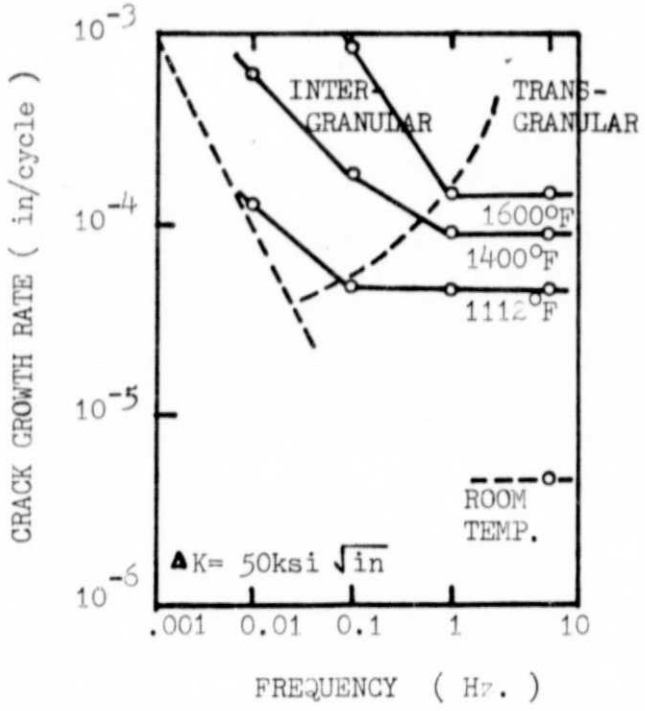

FIG. 7 FREQUENCY AND TEMPERATURE EFFECTS ON FATIGUE CRACK GROWTH RATE OF HS-188 (From Ohmura et al., Ref. A37).

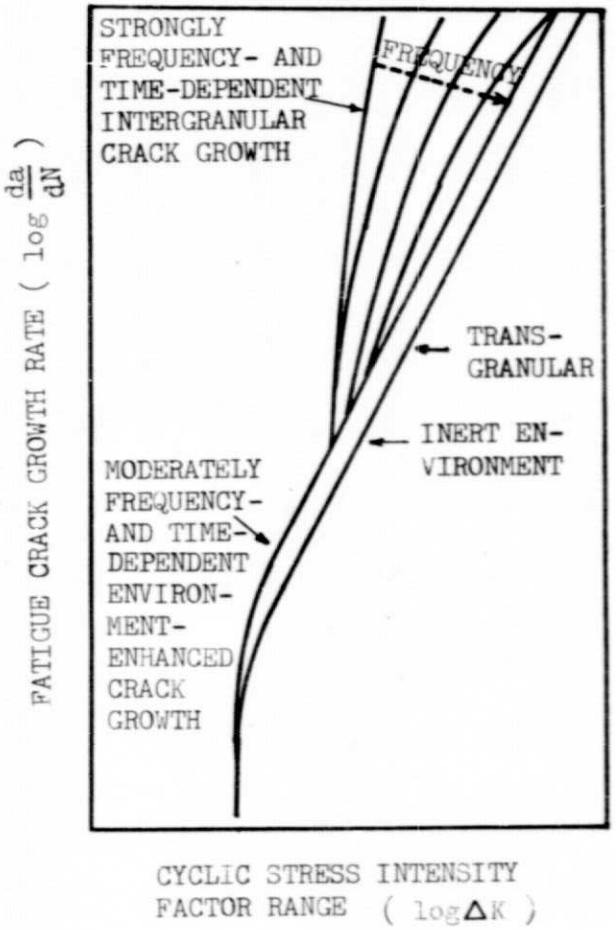

FIG. 8 FREQUENCY EFFECTS ON FATIGUE CRACK GROWTH RATE (From Speidel, Ref. A2).

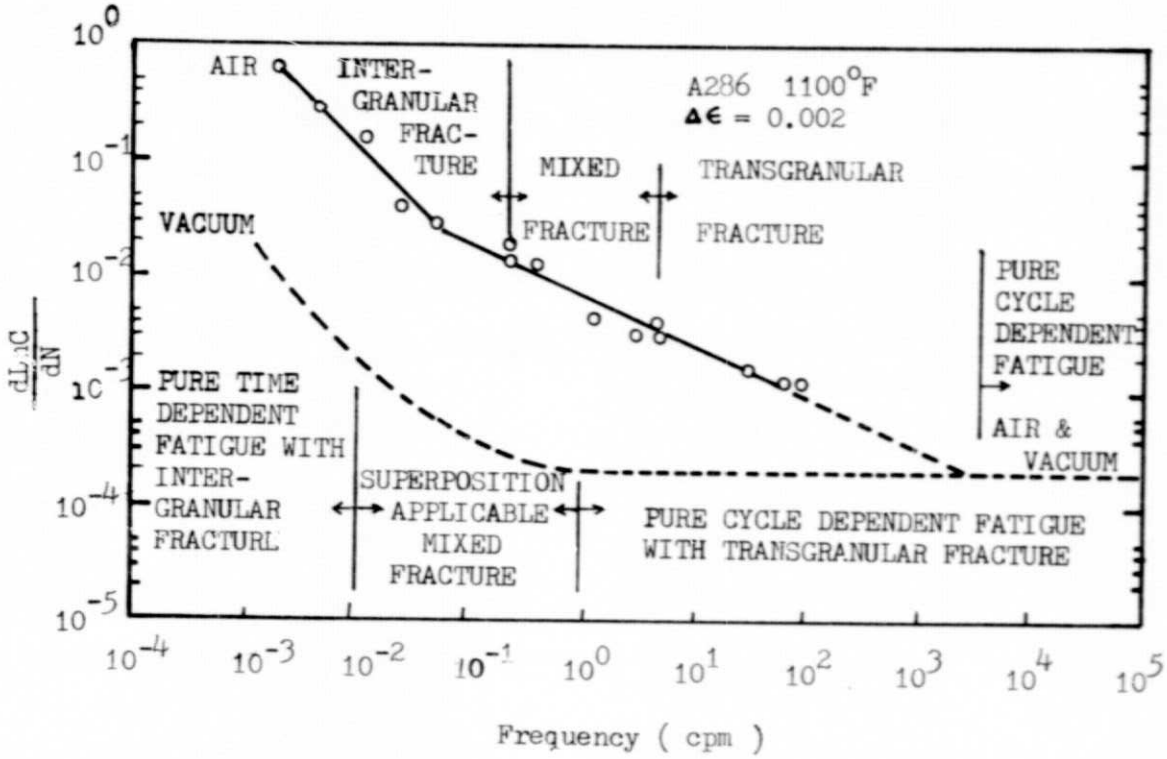

FIG. 9 FREQUENCY EFFECTS ON FATIGUE CRACK GROWTH RATE IN A286, 1100°F (From Solomon et al., Ref. A3).

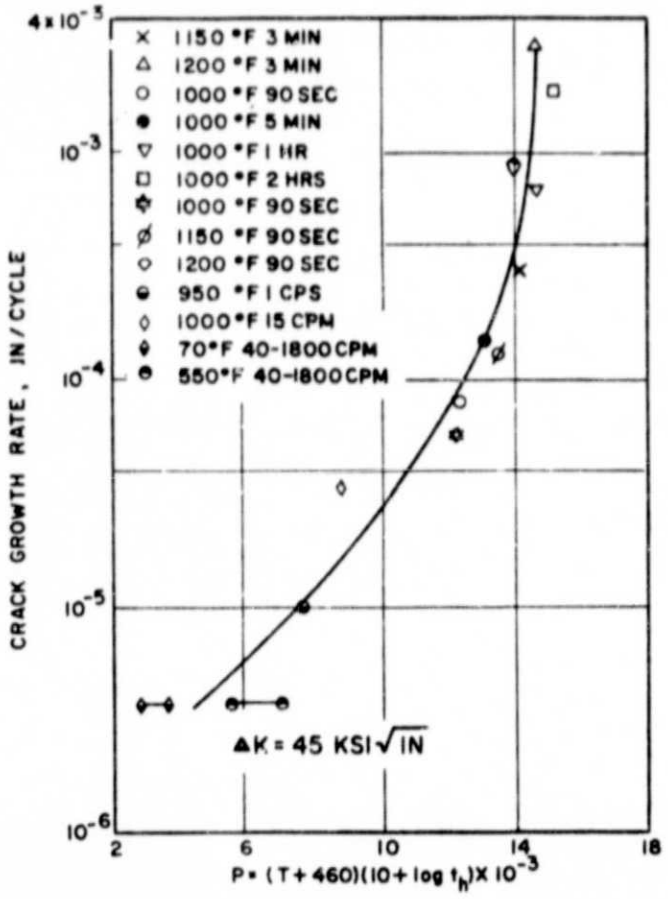

FIG. 10 da/dN VS. LARSON-MILLER PARAMETER FOR CONSTANT ΔK (From Popp et al., Ref. A40).

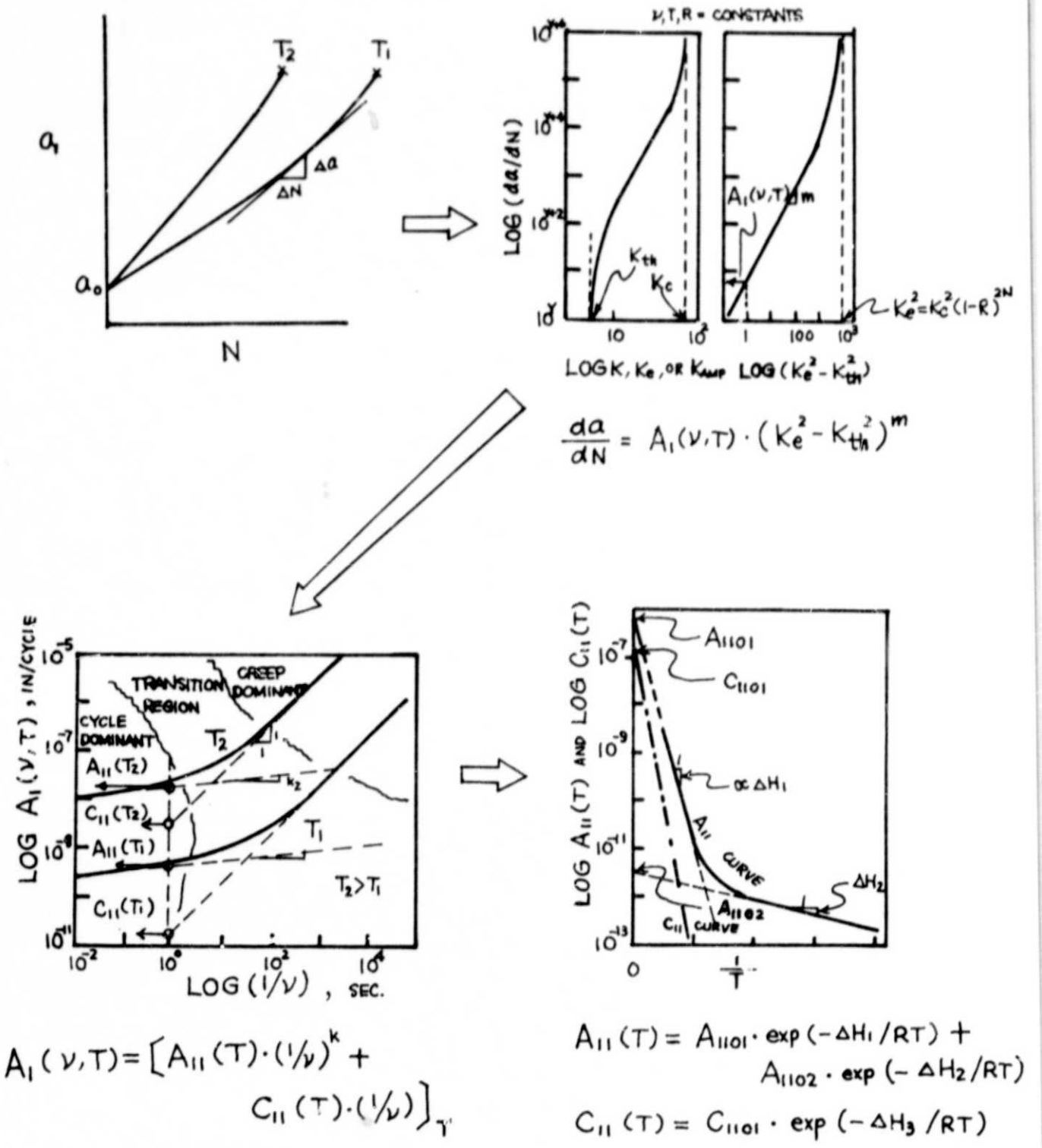

FIG. 11 DERIVATION OF CARDEN'S PARAMETRIC RELATIONSHIP FOR FATIGUE CRACK GROWTH RATE (From Carden, Ref. A41).